PHYSICAL REVIEW A **81**, 013813 (2010)

Glucose concentration measured by the hybrid coherent anti-Stokes Raman-scattering technique

Xi Wang, Aihua Zhang, Miaochan Zhi, Alexei V. Sokolov, and George R. Welch
Department of Physics and Institute for Quantum Studies, Texas A&M University, College Station, Texas 77843, USA
(Received 23 June 2009; published 20 January 2010)

We investigate the possibility of using a hybrid coherent anti-Stokes Raman scattering technique for noninvasive monitoring of blood glucose levels. Our technique combines instantaneous coherent excitation of several characteristic molecular vibrations with subsequent probing of these vibrations by an optimally shaped, time-delayed, narrowband laser pulse. This pulse configuration mitigates the nonresonant four-wave mixing background while maximizing the Raman-resonant signal and allows rapid and highly specific detection even in the presence of multiple scattering. Under certain conditions we find that the measured signal is linearly proportional to the glucose concentration due to optical interference with the residual background light, which allows reliable detection of spectral signatures down to medically relevant glucose levels.

DOI: 10.1103/PhysRevA.81.013813 PACS number(s): 42.65.Dr, 42.65.An, 87.64.kp, 87.14.Df

I. INTRODUCTION

Inelastic scattering of photons by vibrating molecules constitutes the Raman effect, which has become an indispensable tool for analyzing the composition of liquids, gases, and solids [1,2]. Both ordinary Raman spectroscopy and coherent anti-Stokes Raman-scattering (CARS) spectroscopy find widespread use in medical diagnostics [3,4]. While the probability of spontaneous Raman scattering depends on the molecular concentration linearly, for its coherent counterpart—CARS—the signal is known to scale quadratically with the concentration of scatterers due to constructive interference of the resultant coherent photons [1,2]. In recent work, Dogariu *et al.* [5] have measured a clear quadratic dependence of the CARS signal in a variety of samples, including highly scattering powders such as dipicolinic acid, calcite, and gypsum.

Even though CARS may be far superior to spontaneous Raman scattering when the number of scattering molecules is large, at low concentrations the quadratic dependence of CARS is considered to be a disadvantage. In this article we show that under certain conditions the CARS signal can scale linearly with concentration. Motivated by the possibility of noninvasive monitoring of blood glucose levels, we study aqueous glucose solutions and solutions of glucose dissolved in blood. We use a recently developed variant of CARS, termed hybrid CARS [6], which combines broadband pulsed preparation of molecular coherence with frequency-resolved detection via a time-delayed probe, thereby combining the advantages of frequency- and time-resolved spectroscopic techniques [5–8]. The same method of short-pulse excitation and time-delayed narrowband probing was developed as early as 1980 by Zinth [9], with the aim of improving the spectral resolution of CARS beyond the limit of the homogeneous linewidth. Similar mixed time-frequency methods have recently been realized by other groups [10]. Our work on hybrid CARS has been based on our earlier experience with IR, visible, and UV coherent Raman spectroscopy [11]. In the way hybrid CARS mitigates the four-wave mixing background, it shows potential for spectroscopy of highly scattering media such as human tissue.

Although it is known that a resonant signal interfering with a nonresonant background can produce a linear scaling with concentration [12,13], here we observe this effect with the "hybrid CARS" setup described previously. This is important because the setup not only provides background discrimination but also signal amplification, and it does so in a way that provides robust detection of several vibrational modes simultaneously. Furthermore, even though numerous background suppression techniques exist, to the best of our knowledge, in the past the ability to precisely adjust the amplitude and phase of coherent nonresonant background was not used for signal manipulation and amplification. This article shows how this can be done in a system of current practical interest.

II. EXPERIMENTAL SETUP

Figure 1 shows our experimental setup. We employ a Ti:sapphire regenerative amplifier (Coherent Legend, 1 kHz rep. rate, ~1 mJ/pulse) with two evenly pumped optical parametric amplifiers (OPAs) (Coherent OPerA-VIS/UV and OPerA-SFG/UV). These two OPAs provide the pump and Stokes pulses with wavelengths of 1290 nm (full width at half maximum, FWHM, 50 nm) and 1510 nm (FWHM, 70 nm), respectively. The frequency difference between the pump and Stokes beams is approximately 1100 cm^{-1}, which optimizes the excitation of the strong Raman lines in the glucose solution (see Fig. 2). The probe pulse is obtained when the residual fundamental pulse from the second OPA passes through a homemade pulse shaper consisting of a pair of gratings to expand the spectrum in space and a slit to pick a narrow spectral band. The probe beam then has a top-hat-like spectrum at 806 nm with width approximately 1.2 nm (15 cm^{-1}). The probe width is chosen to be comparable with the spectral width of the vibrational modes (around 20 cm^{-1} for glucose) for the purpose of multiplex CARS detection as described in Ref. [6].

These three pulses have parallel polarization and their time overlap is controlled by two translation stages (DS1 and DS2 in Fig. 1). They overlap at their focuses either in a crossing-beam configuration (Figs. 3, 4, and 7) as in Fig. 1

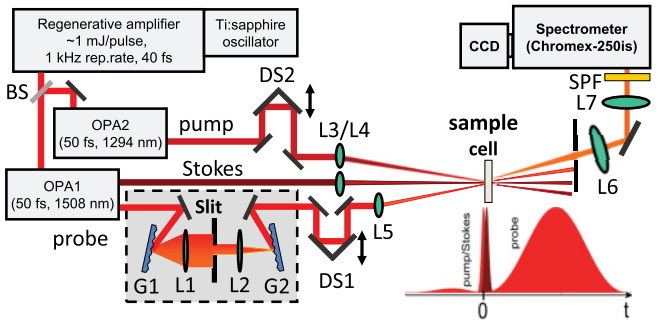

FIG. 1. (Color online) Schematics of the forward CARS setup for glucose detection. BS, beam splitter; G1/G2, grating; L1–L7, lens; DS1/DS2, delay stage; SPF, short-pass filter.

or in a collinear configuration (Figs. 5 and 6). In our case, these two configurations produce similar results and detection sensitivity. D-Glucose solution samples are held in a 2-mm-thick fused silica cell. For the blood samples we use a thinner cell with a thickness of 1 mm for better transmission. The generated CARS signal is collected in a forward geometry and focused onto the entrance slit of the spectrometer (Chromex Spectrograph 250 is) with a liquid-nitrogen-cooled charge-coupled device (CCD) (Princeton Instruments, Spec-10) attached. Typical pulse energy is around a few hundred nanojoules to a few microjoules under different focusing conditions. Because multiple reflections from the front and back of the active layer of the CCD interfere, these surfaces effectively form an etalon which produces a modulation in the recorded spectrum (etaloning). We eliminate this modulation by recording a reference spectrum from the broadband signal generated from a cell with water and dividing the signal spectrum by this reference. This procedure introduces additional noise. A CCD exposure time of a few hundred milliseconds to a few tens of seconds is used to adapt the signal intensity to the dynamic range of the CCD.

III. RESULTS AND DISCUSSION

A. Raman spectra

D-Glucose was obtained from Sigma-Aldrich with purity greater than 99.5%. It was dissolved in distilled water, producing solutions with concentrations varying from 0.02 to 2680 mM (which is slightly below saturation). The D-glucose solutions were prepared a few days before the measurements, in order to reach the anomeric equilibrium. Figure 2 shows Raman spectra from glucose powder and solutions. Due to changes of the anomeric effect and the intramolecular hydrogen bonds [14], the Raman spectra of the D-glucose aqueous solution in Fig. 2(b) are different from that of glucose powder in Fig. 2(a). The D-glucose solution shows two strong and broad Raman lines near 1100 cm^{-1} with spectral FWHM around 20 cm^{-1}, while the other Raman lines at around 850 cm^{-1} and 1350 cm^{-1} are suppressed. We also observe the Raman peaks from water [15]: a narrow line at 1630 cm^{-1}, a strong line below 200 cm^{-1}, and a broad line at 500 cm^{-1}, all of which are comparable with those from glucose. This leads us to choose a frequency difference (pump-Stokes) for our CARS measurements of approximately 1100 cm^{-1} to coherently excite the stronger Raman lines of glucose while avoiding the background from water.

B. CARS spectra

A simple description of the CARS signal generation is through the third-order polarization which can be written as the sum of the background and resonant contributions [16]:

$$P^{(3)}_{\mathrm{CARS}}(\omega) = P^{(3)}_{B}(\omega) + P^{(3)}_{R}(\omega) = \int_0^{+\infty} d\Omega\left[\chi^{(3)}_{B} + N\chi^{(3)}_{R}(\Omega)\right]E_{\mathrm{pr}}(\omega-\Omega)S(\Omega), \tag{1}$$

$$S(\Omega) = \int_0^{+\infty} d\omega' E_p(\omega')E^*_S(\omega'-\Omega), \tag{2}$$

where $E_{\mathrm{pr}}(\omega)$ is the probe field; $S(\Omega)$ is the convolution of the pump field $E_p(\omega)$ and the Stokes field $E_S(\omega)$; and N is the concentration of the Raman active molecule. Most often,

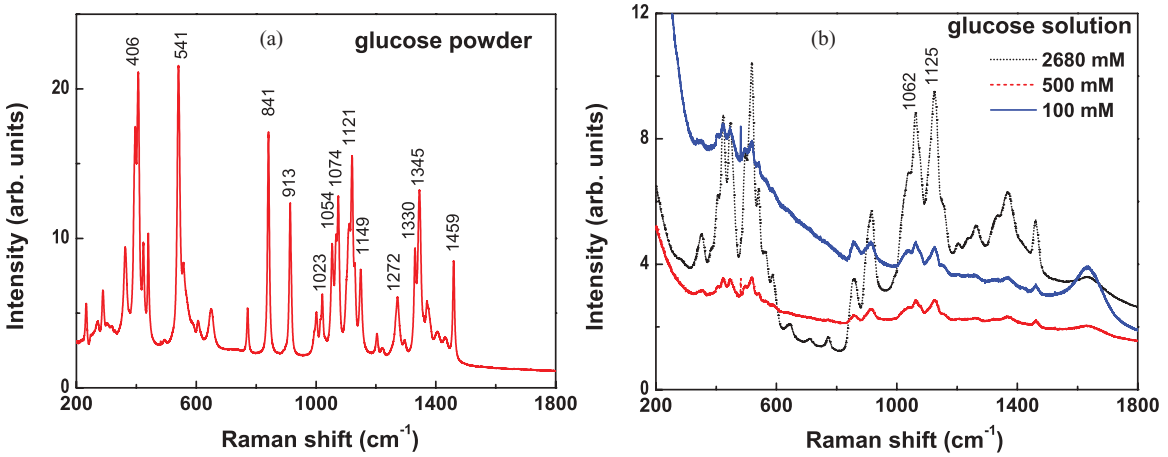

FIG. 2. (Color online) Spontaneous Raman spectra of D-glucose powder (a) and aqueous solutions (b). Data were taken with a 532-nm laser and different experimental parameters.

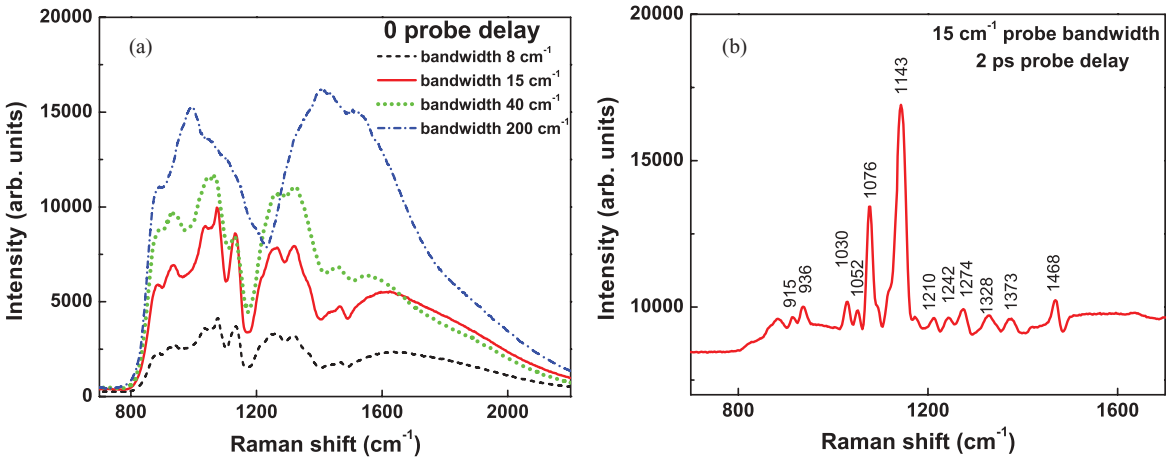

FIG. 3. (Color online) CARS spectra of D-glucose solution at 2680 mM. (a) Spectra at 0 probe delay with different probe bandwidths and the same power; (b) background suppression when probe is delayed to the node; note that the background level is still around 9000 units. Here the integration time is 0.2 s.

although not always, $\chi_B^{(3)}$ corresponds to the nonresonant response and is purely real while the resonant susceptibility $\chi_R^{(3)}$ is complex and, for the case of Lorentzian lineshape, can be written as

$$\chi_R^{(3)}(\omega) = \sum\nolimits_j \frac{A_j}{\Omega_j - \omega - i\Gamma_j}, \tag{3}$$

where $\omega = \omega_{\text{pump}} - \omega_{\text{Stokes}}$; A_j, Ω_j, and Γ_j are the amplitude, frequency, and spectral half width of the jth vibrational mode, respectively. The total CARS signal is given by

$$I_{\text{CARS}}(\omega) \propto \left|P_{\text{CARS}}^{(3)}(\omega)\right|^2 = \left|P_B^{(3)}\right|^2 + \left|P_R^{(3)}(\omega)\right|^2 + 2\text{Re}\left[P_B^{(3)} P_R^{(3)^*}(\omega)\right]. \tag{4}$$

The background component $|P_B^{(3)}|^2$ limits the sensitivity of the CARS measurements. We successfully suppress the nonresonant background by delaying the probe pulse, taking advantage of the instantaneous response of the nonresonant background and the longer lifetime of the resonant vibrations. Theoretically, our probe-pulse intensity has a sinc-squared function profile in the time domain corresponding to the top-hat spectrum. When we delay the probe pulse to make the pump and Stokes pulses overlap with the node of the sinc function (see the inset of Fig. 1), the nonresonant background will be greatly reduced while the resonant signal will remain. However, in practice the background suppression is never perfect, and especially at low concentration of the target molecules the residual background often interferes with the CARS signal. From Eq. (1) we also can see that the bandwidth of the CARS signal peak is determined by the probe bandwidth and the bandwidth of the vibrational mode, whichever is larger. Therefore a narrowband probe is necessary for multiplex CARS to distinguish multiple Raman lines.

C. Probe bandwidth

Figure 3 shows how our setup works for the glucose aqueous solution with a concentration of 2680 mM. Figure 3(a) demonstrates the effect of probe bandwidth at zero probe delay, that is, when the pump and Stokes pulses overlap the peak of the probe pulse. When the probe bandwidth is narrower than that of the glucose modes (around 20 cm^{-1}), we can see the fine features of multiple Raman peaks. This is seen in the dashed and solid (black and red in the color version online) curves for probe bandwidths of 8 and 15 cm^{-1}, respectively.

The resolutions of the Raman lines in these two curves are almost the same. If the probe spectrum is broader, the details of the peaks are obscured, as seen in the dotted and dash-dotted (green and blue) curves with probe bandwidths of 40 and 200 cm^{-1}, respectively. In Fig. 3(b), when the probe is delayed so that its first node overlaps the Stokes and pump pulses, multiple Raman lines stand out against a weak background, in contrast to the solid (red) curve in Fig. 3(a) where the background dominates. However the background suppression is only partial. Even for the strongest peaks in Fig. 3(b), the background is still greater than the signal. The CCD integration time for these spectra is 0.2 s, and the recorded spectral range is approximately 1000 cm^{-1}.

Experimentally we find that the measurement is optimized when the probe bandwidth is comparable to the spectral width of the vibrational modes. Under these conditions, the first node of probe-pulse shape (for 15 cm^{-1} bandwidth) is at 2 ps, while the decay time of glucose modes derived from the spontaneous spectrum in Fig. 2(b) is around 1 ps.

D. Concentration dependence

We have measured CARS signal as a function of glucose concentration in aqueous solution. In these measurements, we delay the probe pulse until its first temporal node overlaps the pump and Stokes pulses. We calculate the intensity of a CARS peak by area integration. In Fig. 4(a), Raman lines at 1143 and 1076 cm^{-1} both show a linear dependence of the signal intensity on the glucose concentration below 1000 mM, with a slope around 1.02 in the log-log scale. In Fig. 4(b) at another probe delay (1.83 ps) the linear fits with slopes 0.98 and 0.95 confirm the linear dependence. This dependence is in

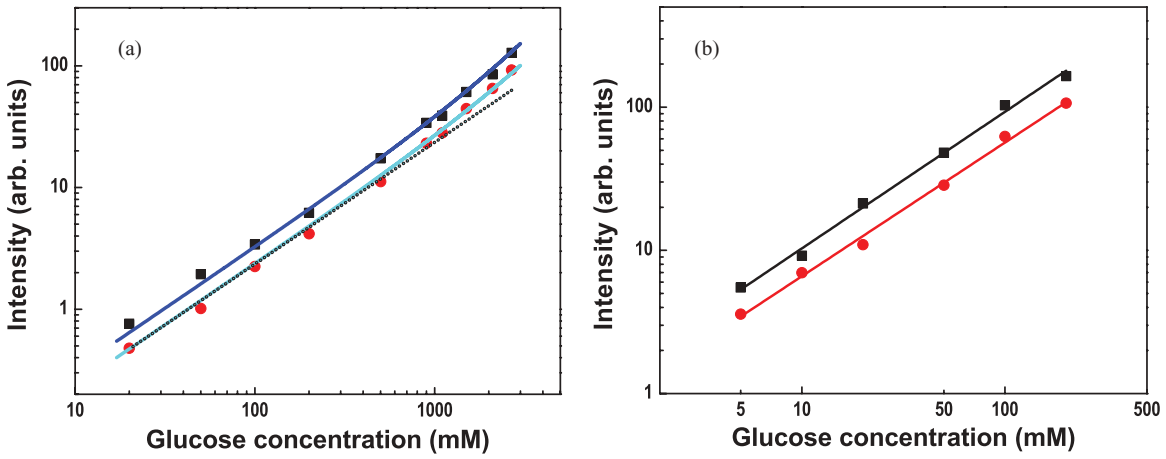

FIG. 4. (Color online) Nearly linear dependence of CARS signal intensity on D-glucose concentration: (a) at 2.00-ps probe delay; (b) at 1.87-ps probe delay. Square and round dots are experimental data of the Raman lines at 1143 and 1076 cm^{-1}, respectively. In panel (a), the solid curves are second-order polynomial fits, and the dotted line has a slope of 1. In panel (b), the best power-law fits have slopes of 0.98 ($\pm$0.03) and 0.95 ($\pm$0.03) for the square and round dots, respectively.

sharp contrast to the quadratic dependence obtained by other groups [5].

As we can see from Eqs. (1) and (4), when the background is suppressed with $P_B^{(3)} = 0$, then we have $I_{\mathrm{CARS}}(\omega) \propto |P_R^{(3)}(\omega)|^2 \propto N^2$. The linear dependence on N observed here thus indicates incomplete suppression of the background. If the residual background is comparable to or larger than the signal of interest $[P_B^{(3)} \geqslant P_R^{(3)}(\omega)]$, then a heterodyne-like product $I_{\mathrm{CARS}}(\omega) \propto 2\mathrm{Re}[P_B^{(3)} P_R^{(3)^*}(\omega)] \propto N$ dominates the weaker resonant signal from glucose. (In our case, this background may be due to a far-detuned CARS signal from water. This is supported by noting that the spontaneous Raman spectra of glucose solutions in Fig. 2 show that the wing of the broad Raman line from water at 500 cm^{-1} crosses the spectral region studied here around 1100 cm^{-1}.) To be more precise, when both contributions are taken into account, we can use a second-order polynomial function $I_{\mathrm{CARS}} = 2E_B E_R(N = 1\ \mathrm{mM})N + [E_R(N = 1\ \mathrm{mM})N]^2$ to fit the experimental data, where E_B is the background electric field magnitude, $E_R(N = 1\ \mathrm{mM})$ is the Raman-resonant electric field contribution per 1 mM glucose, and N is the glucose concentration measured in millimolar. For the two curves (corresponding to the two Raman lines at 1143 and 1076 cm^{-1}) the fitting parameter E_B is taken to be the same, thus constricting the fit. For the two fitting curves, the ratio of the two best-fitting parameters $E_R(N = 1\ \mathrm{mM})$ is found to be equal to 1.36, which is consistent with the observed spectra [Fig. 3(b)]. We can see that the two curves deviate from the dotted line with a slope of 1 at high glucose concentrations (above 1000 mM). Here we would like to mention that in a different experiment with an all-collinear beam configuration, using the same sample cell and the same set of wavelengths, we also obtain a linear dependence of the CARS signal on glucose concentration. We conclude that it is the aforementioned heterodyne effect that gives rise to the linear concentration dependence of the measured signal, and not some sort of loss of optical field coherence. This effect may be beneficial for detection of species at low concentrations.

Quite remarkably, when we reduce the probe-pulse delay such that the background is somewhat increased (and CARS is stronger too), we obtain an overall better performance and are able to reliably detect glucose at lower concentrations. This is demonstrated in Fig. 4(b), which shows the CARS signal from the 1067 and 1143 cm^{-1} lines [similar to those seen in Fig. 4(a)] for a somewhat optimized probe-pulse delay and a lower range of concentration. These data show that the hybrid CARS technique is useful for optimizing (and not only maximizing) the signal-to-background ratio and allows us to take full advantage of the aforementioned heterodyne amplification. Although increasing the background even more would introduce extra noise, we can detect glucose signals down to 5 mM in concentration, which is medically relevant and demonstrates the power of this technique.

E. Glucose measurement in blood

We have also measured CARS signals from glucose dissolved in pig blood. Figure 5 shows several spectra in the region of interest for different concentrations of glucose. It is apparent that the strong glucose lines seen in aqueous solution are still present, but that other features are also present that were not seen in aqueous solution.

For the data shown in Fig. 5, the samples of pig blood were prepared by adding different volumes of highly concentrated glucose solution into a fixed volume of pig blood. In Fig. 5(a), the signal intensity at 1015 cm^{-1} decreases as more glucose solution is added, while the glucose lines previously observed increase. Furthermore, this line disappears in a pure glucose solution. This shows that the constituent corresponding to the Raman line at 1015 cm^{-1} is diluted more when more glucose solution is added, and the linear decrease of the intensity of this Raman line on the volume of glucose solution [see Fig. 5(b)] shows that this constituent corresponds to a component in blood, not water or glucose. This allows us to use this Raman line as a reference. That is, we can measure the ratio of the height of a glucose line to this peak, in order to help eliminate distortion arising from laser intensity fluctuations.

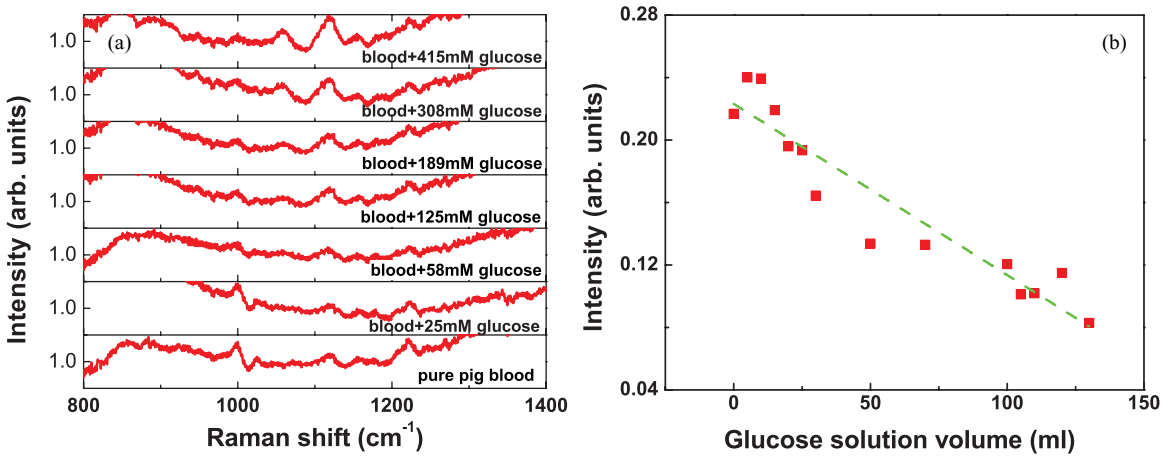

FIG. 5. (Color online) (a) CARS spectra of pig blood. The mixtures were obtained by adding different volumes of glucose solution into blood with fixed volume. In each case, the ordinate scale is from 0.8 to 1.2. (b) Linear decrease of the reference signal at 1015 cm^{-1} on the glucose volumes added into blood in panel (a).

Furthermore, we note that we can see the reference signal and the weak CARS signals from glucose even in pure blood.

Figure 6 shows the CARS signal from the 1143 cm^{-1} glucose line in blood. In Fig. 6(a), the intensity is nearly linearly dependent on the glucose concentration, but fluctuations are seen at low concentrations. Figure 6(b) shows the ratio of this glucose peak to the reference peak. This ratio increases along a smooth curve (nearly a line) when the glucose concentration goes up. We can clearly distinguish the glucose concentrations over 10 mM. The flattening of this curve at low concentration may be due to the naturally occurring glucose in the pig blood that was used. Thus with the aid from the reference signal, the measurement sensitivity is highly enhanced. Although better sensitivity is still needed for practical applications, our method shows promise for low-concentration detection.

F. Phase changes in CARS signals

We have observed an interesting phenomenon: the phase of the generated CARS field changes when we delay the probe pulse, as shown in Fig. 7. Figure 7(a) shows the temporal profile of the probe pulse, as measured through four-wave mixing (FWM) in water with pump and Stokes pulses. For these data, the first node occurs 2.0 ps after the peak of the probe pulse. When this node coincides with the arrival of the pump and Stokes pulses, the resultant anti-Stokes spectrum is dominated by the Raman lines of glucose and is nearly background free (for high glucose concentrations), as shown in Fig. 3(b). When the first node of the probe pulse comes before the pump and Stokes pulses, the spectrum shows Raman lines with dip structures, as seen in the dotted (blue in color) curve in Fig. 7(b). When the delay is greater than 2.0 ps, peaks are seen, as in the solid (red) curve in Fig. 7(b). We attribute this phase change to the fact that the probe field changes phase as it goes through a node, similar to the Gouy phase shift of an electromagnetic field propagating through a focus. Real-world applications based on this type of delayed-pulse scheme will have to accurately account for this effect in order to model the CARS line shapes.

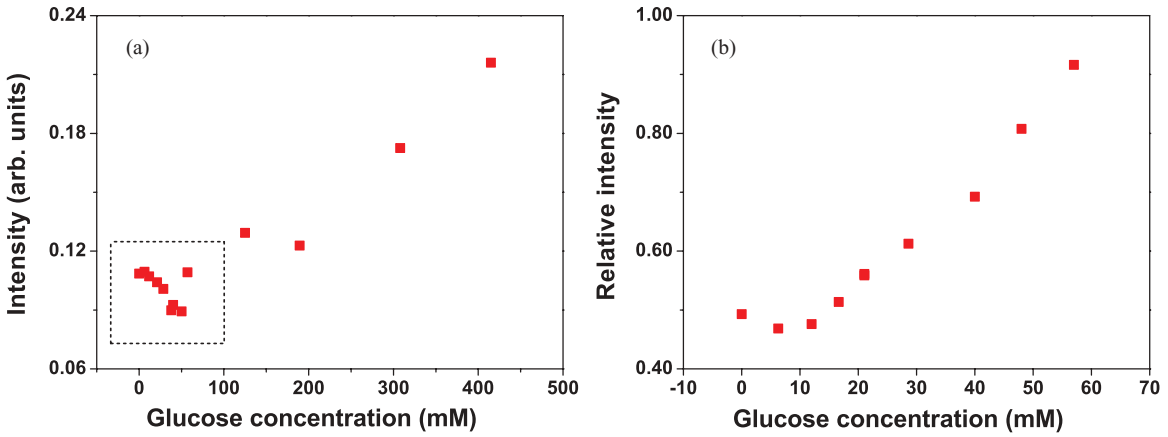

FIG. 6. (Color online) (a) CARS signal from 1143 cm^{-1}. We observe an approximately linear dependence with concentration. The noise at low concentration is due to laser intensity fluctuation. (b) Ratio of glucose CARS signal at 1143 cm^{-1} to reference line from blood for the boxed area in panel (a).

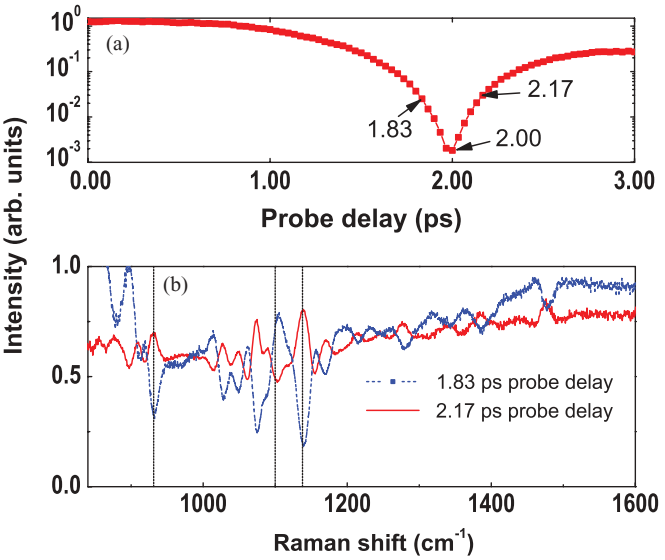

FIG. 7. (Color online) (a) Temporal profile of the probe beam, as measured through FWM in water with pump and Stokes pulses; (b) CARS spectra of 500 mM glucose solution at 1.83- and 2.17-ps probe delays.

IV. CONCLUSION

In this article, we demonstrated the application of a hybrid CARS technique to highly precise, noninvasive glucose detection. We obtained CARS spectra from both pure glucose solutions and from blood samples. We found a linear dependence of the CARS signal on the glucose concentrations due to interference between the resonant signal and the broad off-resonant background from water. Our method is reliably capable of measuring glucose samples with concentrations as low as 5 mM. Furthermore, our method is also optimized for multiplex CARS and thus allows chemical specifications.

We have demonstrated how interference between signal and background gives rise to a linear dependence of signal on concentration, and we have shown how the phase of the probe field affects this. In our experiment the background amplitude was adjusted by variable probe-pulse delay and the background phase was varied due to the Gouy-like phase change around the temporal node of the probe field. Even though in this experiment the amplitude and phase were not varied independently, in principle their independent control is possible though slightly more elaborate probe-pulse shaping. Therefore, this work shows how essentially the full range of heterodyne CARS capabilities can be achieved in a simple configuration (not involving an interferometer) where the fully controllable local oscillator (background) field is obtained from the same sample.

ACKNOWLEDGMENTS

We thank Marlan O. Scully for many useful and stimulating discussions and for providing much of the equipment used in these experiments. We thank Jaan Laane for helpful discussion and Kathleen McCann for their generous assistance with spontaneous Raman measurements. We gratefully acknowledge support from Aretais, Inc, the Office of Naval Research, the National Science Foundation (Grants PHY 354897 and PHY 722800), the Texas Advanced Research Program (Grant 010366–0001-2007), the Army Research Office (Grant W911NF-07–1-0475), and the Robert A. Welch Foundation (Grant A1547).

[1] H. A. Szymanski, *Raman Spectroscopy* (Plenum, New York, 1967).
[2] G. L. Eesley, *Coherent Raman Spectroscopy* (Pergamon, New York, 1981).
[3] R. Petry, M. Schmitt, and J. Popp, ChemPhysChem **4**, 14 (2003).
[4] C. Evans and X. S. Xie, Annu. Rev. Anal. Chem. **1**, 883 (2008).
[5] A. Dogariu, A. Goltsov, H. Xia, and M. O. Scully, J. Mod. Opt. **55**, 3255 (2008).
[6] D. Pestov, R. K. Murawski, G. O. Ariunbold, X. Wang, M. Zhi, A. V. Sokolov, V. A. Sautenkov, Y. V. Rostovtsev, A. Dogariu, Y. Huang, and M. O. Scully, Science **316**, 265 (2007).
[7] D. Pestov, X. Wang, G. O. Ariunbold, R. K. Murawski, V. A. Sautenkov, A. Dogariu, A. V. Sokolov, and M. O. Scully, Proc. Natl. Acad. Sci. U.S.A. **105**, 422 (2008).
[8] A. Dogariu, A. Goltsov, D. Pestov, A. V. Sokolov, and M. O. Scully, J. Appl. Phys. **103**, 036103 (2008).
[9] W. Zinth, Opt. Commun. **34**, 479 (1980).
[10] B. D. Prince, A. Chakraborty, B. M. Prince, and H. U. Stauffer, J. Chem. Phys. **125**, 044502 (2006).
[11] D. Pestov, M. Zhi, Z. E. Sariyanni, N. G. Kalugin, A. A. Kolomenskii, R. K. Murawski, G. G. Paulus, V. A. Sautenkov, H. Schuessler, A. V. Sokolov, G. R. Welch, Y. V. Rostovtsev, T. Siebert, D. A. Akimov, S. Graefe, W. Kiefer, and M. O. Scully, Proc. Natl. Acad. Sci. U.S.A. **102**, 14976 (2005).
[12] R. F. Begley, A. B. Harvey, and R. L. Byer, Appl. Phys. Lett. **25**, 387 (1974).
[13] W. M. Tolles, J. W. Nibler, J. R. McDonald, and A. B. Harvey, Appl. Spectrosc. **31**, 253 (1977).
[14] C. Molteni and M. Parrinello, J. Am. Chem. Soc. **120**, 2168 (1998).
[15] Y. Tominaga, A. Fujiwara, and Y. Amo, Fluid Phase Equilib. **144**, 323 (1998).
[16] D. Oron, N. Dudovich, D. Yelin, and Y. Silberberg, Phys. Rev. A **65**, 043408 (2002).